

Original Research

Dual inhibition of AKT and autophagy sensitizes triple negative breast cancer cells to carboplatin

Jun-zhen Zhou^{a,1}, Jing-ya Wen^{b,1}, Xin-wen Xu^{a,c}, Na Zhao^d, Jing-jing Tang^{a,e}, Ye-rui Xiao^f, Le-yang Xiang^b, Yue Jiang^g, Jian-wei jiang^{d,*}, Hong Hong^{h,*}, Qing Zhang^{a,*}^a Department of Breast Surgery, The First Affiliated Hospital of Jinan University, Guangzhou, Guangdong 510632, China^b Department of General Surgery, The First Affiliated Hospital of Jinan University, Guangzhou, Guangdong 510632, China^c Department of Breast Surgery, Foshan Second People's hospital, Foshan, Guangdong 52800, China^d Department of Biochemistry, Basic Medical College, Jinan University, Guangzhou 510632, China^e Department of Breast and Thyroid Surgery, the Central Hospital of Yongzhou, Yongzhou, Hunan 425000, China^f Department of Stomatology, Stomatological Medical College, Jinan University, Guangzhou, Guangdong 510632, China^g Department of Thyroid and Breast Surgery, Shunde Hospital of Jinan University, Foshan, Guangdong 528303, China^h Department of Breast Surgery, The Hospital of eastern Dongguan, Dongguan, Guangdong 523560, China

ARTICLE INFO

Keywords:

EM-2
Breast cancer
Carboplatin
Autophagy
AKT

ABSTRACT

Triple-negative breast cancer (TNBC) exhibits the highest recurrence and mortality rates among breast cancer subtypes. Approximately one million TNBC cases are diagnosed worldwide annually. Current clinical treatments, primarily chemotherapy regimens based on paclitaxel and anthracycline, are associated with high recurrence rates and low overall survival rates. Platinum drugs, introduced for TNBC treatment, demonstrated a positive effect; however, their high-dose administration inevitably results in toxic side effects and drug resistance. Therefore, identifying agents that sensitize patients to platinum-based therapies is critical. Analysis of the TCGA database revealed that AKT1 and autophagy are activated in breast cancer, playing crucial roles in malignant behavior. Further investigation demonstrated that CBP activates the AKT pathway in MDA-MB-231 cells, while its combination with LY294002 or Triciribine (inhibitors of the PI3K/AKT pathway), suppresses cell proliferation. However, this combination also activates autophagy, a protective mechanism. Inhibition of autophagy with CQ or Baf A1 further increased the proliferation-inhibitory effects of CBP in MDA-MB-231 cells. Notably, the sesquiterpene lactone EM-2 extracted from *Elephantopus mollis* H.B.K., significantly inhibited both the AKT and autophagy pathways in TNBC cells, demonstrating superior cellular inhibitory effects compared with other AKT or autophagy inhibitors combined with CBP. When CBP was combined with EM-2, cell survival decreased by approximately 36 % compared with CBP monotherapy, while the apoptosis rate increased by 22.8 % after 48 h. The combination of CBP and EM2 also produced the greatest tumor shrinkage *in vivo*. Interestingly, the CBP (3 mg/kg) + EM-2 (6 mg/kg) group achieved the same tumor shrinkage, with only one-fifth the amount of CBP compared with the CBP (16 mg/kg) monotherapy group. In other words, low doses of EM-2 combined with CBP produced the same anti-tumor effects as high-dose CBP alone. These findings provide a novel strategy for the treatment of CBP using dual AKT and autophagy inhibitors, highlighting potential clinical applications.

Introduction

Triple-negative breast cancer (TNBC) is characterized by the absence

of estrogen receptor (ER), progesterone receptor (PR), and proto-oncogene HER-2 expression, as determined by immunohistochemical examination of cancer tissue [1,2]. This subtype exhibits the highest

Abbreviations: (CBP), Carboplatin; (TNBC), Triple-negative breast cancer; (ER), estrogen receptor; (PR), progesterone receptor; (CI), combination index; (DMSO), dimethyl sulfoxide; (Baf-A1), Bafilomycin A1; (CQ), chloroquine; (ECL), electrochemiluminescence; (PVDF), polyvinylidene fluoride; (PARP), poly ADP-ribose polymerase; (DDP), cisplatin; (5-Fu), 5-fluorouracil; (PTX), paclitaxel; (H&E), hematoxylin and eosin.

* Corresponding authors.

E-mail addresses: jjw703@jnu.edu.cn (J.-w. jiang), 380419272@qq.com (H. Hong), zq1994@jnu.edu.cn (Q. Zhang).

¹ These authors contributed equally to this work.

<https://doi.org/10.1016/j.tranon.2025.102434>

Received 21 November 2024; Received in revised form 14 May 2025; Accepted 24 May 2025

1936-5233/© 2025 Published by Elsevier Inc. This is an open access article under the CC BY-NC-ND license (<http://creativecommons.org/licenses/by-nc-nd/4.0/>).

recurrence and mortality rates among breast cancers, with approximately 1 million cases diagnosed worldwide annually [1,3,4]. Patients with TNBC undergo various treatments based on cancer type and stage, including chemotherapy, radiotherapy, immunotherapy, laser therapy, photodynamic therapy [5–8]. Early adjuvant and neoadjuvant chemotherapy regimens, predominantly based on paclitaxel and anthracycline, remain the most common interventions. However, these treatments are associated with high recurrence rates, low overall survival, and acute toxic effects—such as irreversible cardiotoxicity and myelotoxicity—that restrict their clinical utility [9–11]. Platinum-containing regimens have emerged as among the most studied and effective TNBC treatments in recent years [12,13]. These agents primarily function by forming DNA adducts, which disrupt DNA replication and transcription, ultimately inducing cell death [14,15]. In clinical practice, however, platinum resistance significantly impairs treatment outcomes, frequently leading to therapeutic failure and disease recurrence [16]. A combined treatment plan may offer an effective solution. For example, the synergistic effect between AKT inhibitors and carboplatin (CBP) has been demonstrated to enhance therapeutic outcomes in cancers such as ovarian, lung, endometrial cancer and uterine serous carcinoma [17–21], despite limitations of AKT inhibitors, including the induction of protective autophagy [22].

The PI3K/AKT pathway ranks among the most frequently over-activated intracellular pathways in numerous human cancers, including breast, lung, head and neck, endometrial, prostate, and colorectal cancers [23,24]. Its activation triggers downstream AKT targets, promoting oncogenesis, proliferation, invasion, and metastasis of tumor cells [23, 25]. Overactivation of the PI3K/AKT/mTOR signaling pathway is observed in approximately 70 % of patients with breast cancer (BC) and 25 % of those with TNBC [26,27]. Inhibition of AKT has been shown to suppress tumor cell growth [23,28,29]. In breast cancer, approvals for ER-positive advanced breast cancer include the PI3K inhibitor alpelisib for PIK3CA-mutated tumours, the AKT inhibitor capivasertib for tumours with alterations in PIK3CA, AKT1, or PTEN, and the mTOR inhibitor everolimus, which is used irrespective of mutation status [30]. And luteolin was reported to inhibit proliferation and metastasis in androgen receptor-positive TNBC by downregulating the AKT/mTOR pathway [31], while calycosin suppressed TNBC progression via the PI3K/AKT signaling pathway [32]. Despite promising preclinical efficacy in some tumor models [33], the clinical response to small-molecule inhibitors of this pathway remains limited, as single AKT inhibition typically induces growth arrest rather than cell death in solid tumors [34]. To enhance AKT inhibitor-mediated cancer cell death, combining drugs has been explored in numerous studies.

In diagnosed tumors, autophagy sustains the survival of cancer cells under metabolic stress conditions, such as hypoxia, nutrient deprivation, and chemotherapy [35–37]. The interplay between autophagy and apoptosis may contribute to platinum resistance, as autophagy can suppress apoptosis response to platinum, thus promoting cell survival [38,39]. Autophagy serves as a survival mechanism in response to platinum-induced stress [40], with aggressive tumors like TNBC exhibiting elevated autophagy levels to tolerate cellular stress during metastasis [41–43]. Moreover, multiple studies have indicated that common PI3K/AKT/mTOR inhibitors can induce autophagy in different preclinical models, facilitating the evasion of their antitumor effects [22,44]. Given the autophagy-induced resistance associated with platinum therapy and the autophagy-promoting effects of conventional PI3K/AKT/mTOR inhibitors, a novel inhibitor capable of simultaneously suppressing both autophagy and the AKT pathway could improve TNBC prognosis.

Natural products are widely applied in tumor treatment due to their low cytotoxicity, high efficiency, and cost-effectiveness. In this study, a sesquiterpene lactone monomer, EM-2, extracted from *Elephantopus mollis* H.B.K., was identified as an inhibitor of both the AKT pathway and autophagy. Combining CBP with EM-2 reduced cell survival by approximately 36 % compared to CBP monotherapy, with the apoptosis

rate increasing by 22.8 % after 48 h. The combination of CBP and EM-2 was also demonstrated to produce the greatest effect on tumor shrinkage *in vivo*.

Results

Upregulation of AKT1 and autophagy-related genes predicts poor prognosis in patients with breast cancer

The Cancer Genome Atlas (TCGA) database was used for pre-processing and screening. Elevated mRNA levels of AKT1, p62, and ATG7 were observed in breast cancer tissues compared to normal tissues (99 cases of adjacent tissues and 1072 cases of tumor tissues; Fig. 1A). Matching analyses further revealed overexpression of AKT1 and autophagy-related genes (p62, ATG5, and ATG7) in cancer tissues relative to paired adjacent breast tissues ($n = 96$; Fig. 1B). Subsequently, Kaplan–Meier analyses were conducted using 1020 cases with complete survival data from the TCGA cohort. Patients were divided into high- and low-risk groups with optimum cutoff values of AKT1 and autophagy-related genes, respectively. High expression levels of AKT1, ATG5, and ATG7 were associated with shorter overall survival (Fig. 1C). In contrast, the expression level of p62 in cancer tissues showed no correlation with overall survival ($P = 0.18$, Fig. 1C). These findings indicate that AKT1 and autophagy are activated in breast cancer and contribute significantly to malignant biological behavior.

Inhibition of the AKT pathway can increase the anti-TNBC effect of CBP but autophagy was activated

Analysis of relevant data from the ATGG database indicated that CBP activates the AKT pathway in TNBC cells following treatment, and that inhibiting this pathway may enhance the anti-TNBC effect of CBP. As shown in Fig. 2A, expression levels of p-AKT Ser473, p-AKT Thr308, p-GSK3 β , p-FOXO3, and p-MDM2 increased with rising CBP concentration, confirming activation of the AKT pathway in MBA-MD-231 cells. When cells were pretreated with LY294002, a PI3K/AKT pathway inhibitor, expression levels of p-AKT Ser473 and p-AKT Thr308 were reduced, as were those of the downstream AKT proteins p-GSK3 β and p-FOXO3, compared to cells treated with CBP alone (Fig. 2B). p62, a widely studied autophagy substrate, exhibits an inverse correlation between its protein expression and autophagy activity during autophagosome formation [45]. In the LY294002 + CBP group, p62 expression was reduced, suggesting the activation of the autophagic in MDA-MB-231 cells. Furthermore, MTT and EdU experiments demonstrated that inhibition of the AKT pathway enhanced the inhibitory effect of CBP on MDA-MB-231 cells (Fig. 2C, D).

Inhibition of autophagy enhances the anti-breast cancer effect of CBP

Autophagy is involved in the catabolic processes that promote the degradation of overabundant or malfunctioning cellular components [46]. Increasing evidence suggests that autophagy is associated with poor chemotherapeutic drug treatments. Western blotting was performed to explore the effects of CBP on autophagy. As shown in Fig. 3A, p62 expression decreased with increasing CBP concentration, indicating that autophagy was activated. In MDA-MB-231 cells, cell viability in CBP + CQ or CBP + Baf A1 groups decreased by 22.64 % and 14.87 %, respectively, compared to the CBP group (Fig. 3B). In addition, EdU assay results indicated that blocking autophagic flux with CQ increased the sensitivity of MDA-MB-231 cells to CBP (Fig. 3C). These findings demonstrate that CBP induces protective autophagy, and inhibiting autophagic flux enhances the anti-TNBC effects of CBP.

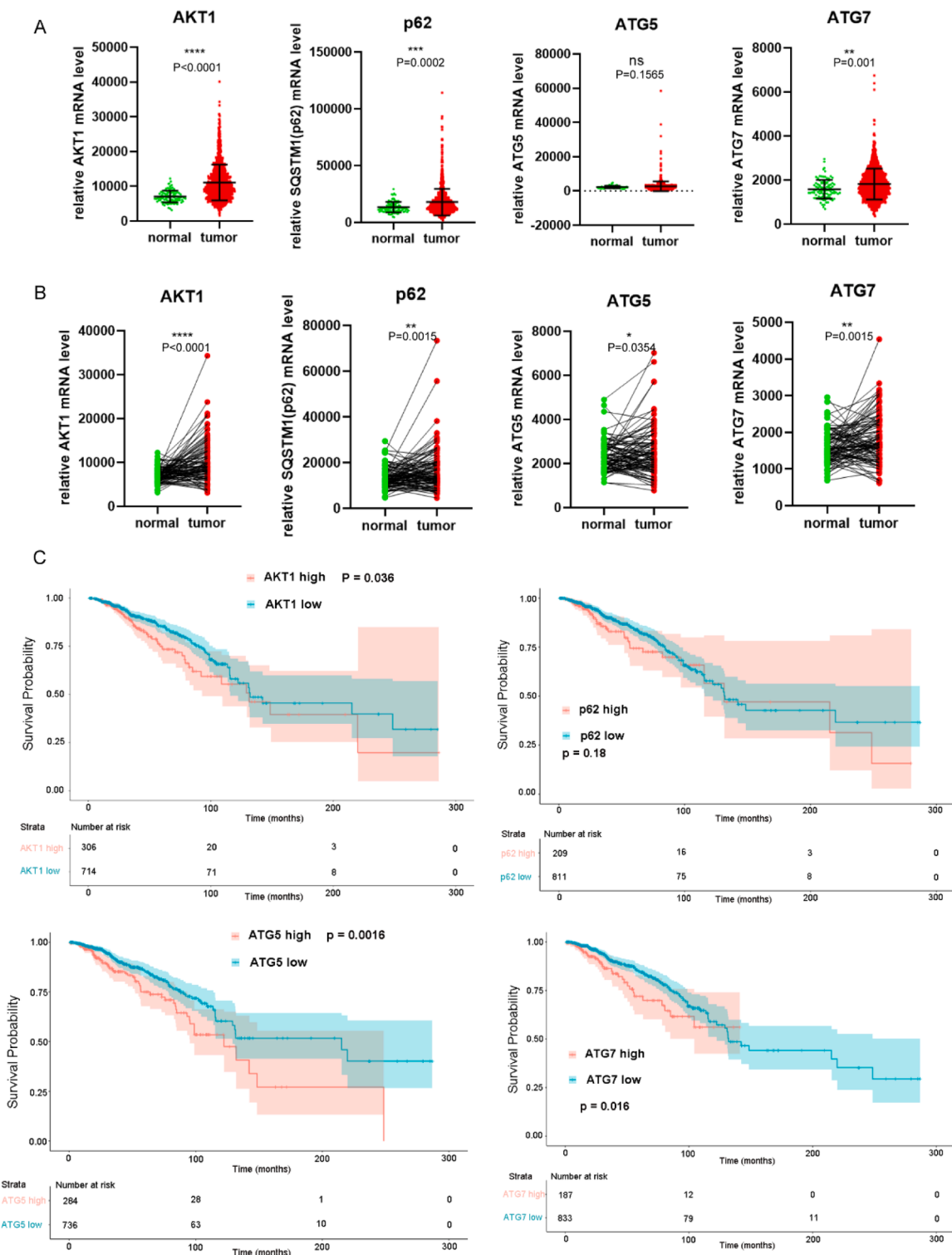


Fig. 1. Upregulation of AKT1 and autophagy-related genes predicts poor prognosis in patients with breast cancer. (A) Elevated mRNA levels of AKT1, p62, and ATG7 (but not ATG5) were observed in breast cancer tissues compared to normal tissues (99 cases of adjacent tissues and 1072 cases of tumor tissues). (B) Overexpression of AKT1 and autophagy-related genes (p62, ATG5, and ATG7) was detected in cancer tissues relative to paired adjacent breast tissues ($n = 96$). (C) Kaplan–Meier analyses were performed on patients with breast cancer, categorized by expression levels of AKT1, p62, ATG5, and ATG7; data were obtained from TCGA breast cancer ($n = 1020$). * $P < 0.05$, ** $P < 0.01$, *** $P < 0.001$, **** $P < 0.0001$, ns, not significant.

CBP combined with EM-2 exhibits a synergistic anti-tumor effect on TNBC cells

The chemical structure of EM-2 is shown in Fig. 4A. In this study, MDA-MB-231 and MDA-MB-468 cells were selected to assess the

growth-inhibitory effects of EM-2 / CBP / EM-2 + CBP over 48 h. Cell viability was detected using a MTT assay (Fig. 4B, C). In both MDA-MB-231 and MDA-MB-468 cells, the inhibitory effect on cell proliferation increased progressively with higher concentrations of CBP and EM-2. MDA-MB-231 and MDA-MB-468 cells treated with EM-2 in

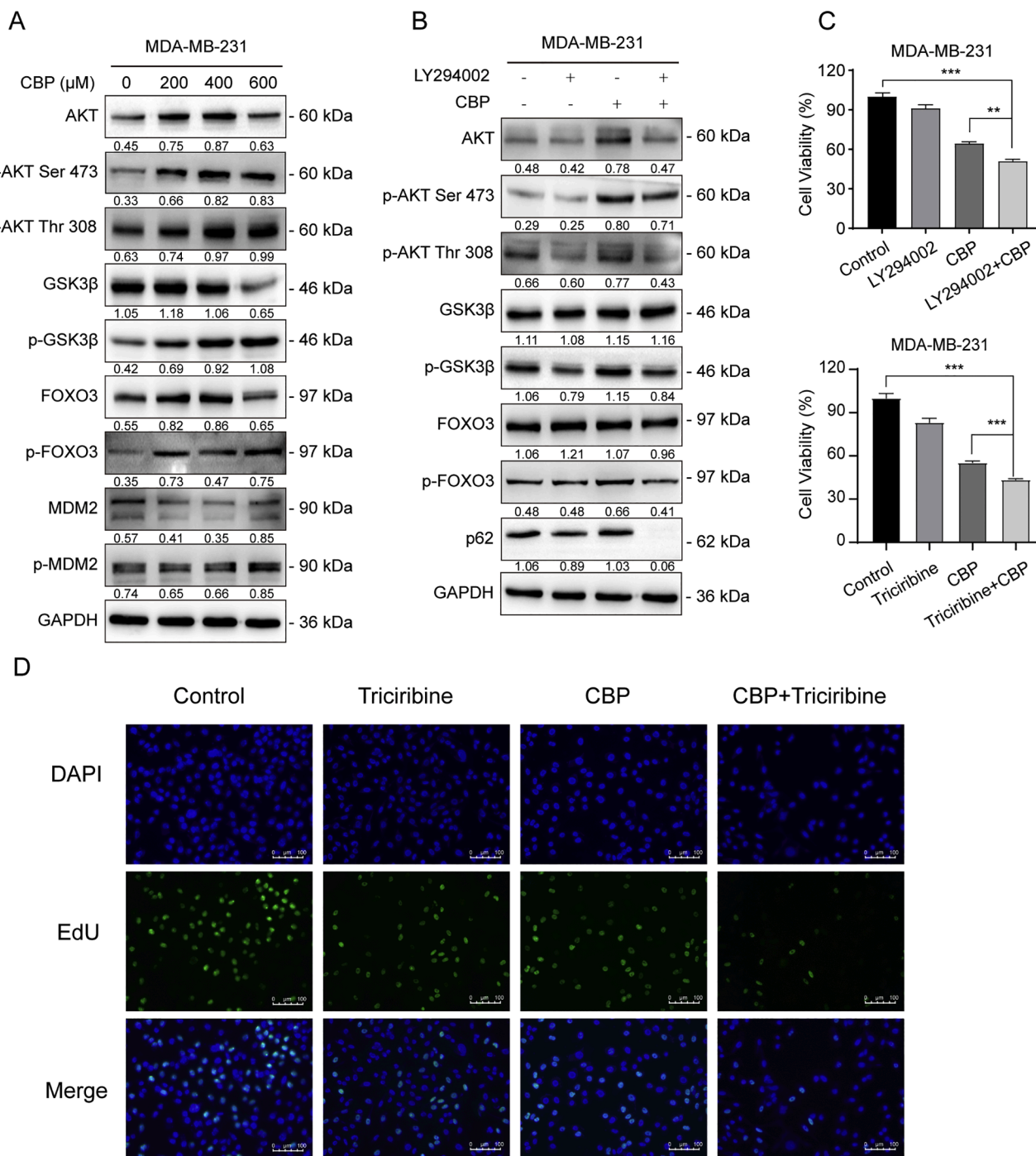


Fig. 2. CBP induces activation of the AKT signaling pathway, and inhibition of this pathway enhances the anti-breast cancer effect of CBP. (A) MDA-MB-231 cells were treated with CBP (0, 200, 400, 600 μM) for 24 h and Western blot analysis was performed to detect the expression level of proteins related to the AKT pathway. (B) MDA-MB-231 cells were treated with CBP (400 μM) for 24 h in the presence or absence of LY294002 (10 μM), and Western blot analysis was performed to detect the expression level of proteins associated with the AKT pathway. (C) MDA-MB-231 cells were treated with CBP (400 μM) for 24 h in the presence or absence of LY294002 (10 μM) or Triciribine (10 μM), and the cell viability was detected by MTT assay (***P* < 0.01, ****P* < 0.001). (D) The cell proliferation inhibitory effect of CBP (200 μM, 24 h) in the presence or absence of Triciribine (10 μM) on MDA-MB-231 cells was detected by EdU assay and DMSO treatment with the largest volume ratio of 0.02 % as the control group.

combination with CBP exhibited combination index (CI) < 1 (Fig. 4D and E), indicating a synergistic effect. This effect was more pronounced in MDA-MB-231 cells.

EM-2 acts as a dual inhibitor of the AKT pathway and autophagy

To investigate the molecular mechanism underlying EM-2

sensitization of CBP, Western blotting was performed to determine the effects of EM-2 on the AKT pathway and autophagic flux in MDA-MB-231 cells. As shown in Fig. 5A, the expression levels of p-AKT Ser 473 and p-AKT Thr308 proteins decreased with increasing concentrations of EM-2 over 24 h, accompanied by reduced phosphorylation of downstream proteins GSK3β and FOXO3. In contrast, levels of cell cycle-related proteins p21 and p27 increased, suggesting that EM-2 also induced

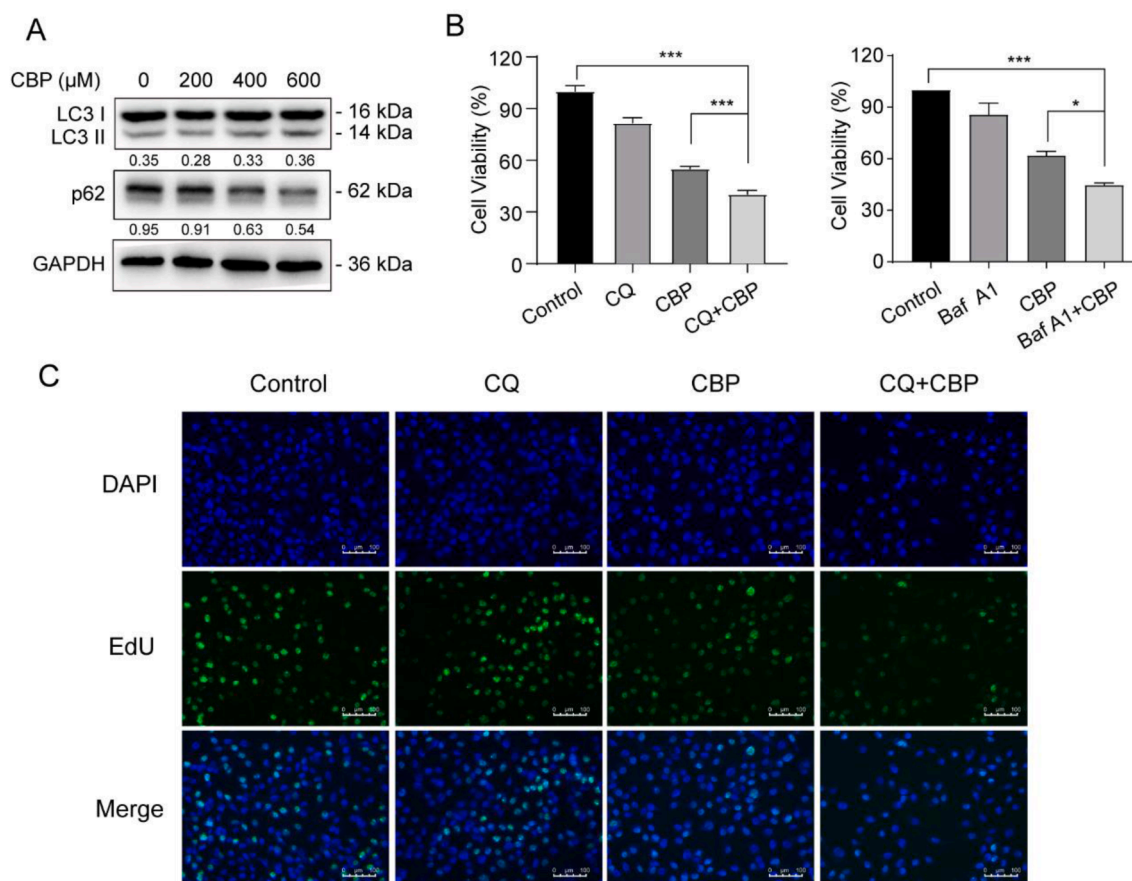


Fig. 3. CBP induces protective autophagy, and inhibition of autophagy enhances the anti-TNBC effect of CBP. **(A)** MDA-MB-231 cells were treated with CBP (0, 200, 400, 600 μM, 24 h), and Western blot analysis was performed to detect the expression level of proteins associated with autophagy. **(B)** MDA-MB-231 cells were treated with CBP (400 μM, 24 h) in the presence or absence of Baf A1 (100 nM) or CQ (10 μM), and MTT analysis was performed to detect the cell viability (* $P < 0.05$, ** $P < 0.01$, *** $P < 0.001$). **(C)** The cell proliferation inhibitory effect of CBP (200 μM, 24 h) in the presence or absence of CQ (10 μM) on MDA-MB-231 cells were detected by EdU assay and DMSO treatment with the largest volume ratio of 0.02 % as the control group.

cell cycle arrest. In a subsequent time-gradient experiment, MDA-MB-231 cells were treated with 5 μM EM-2 for 0, 3, 6, 9, 12, and 24 h, and Western blot analysis was performed (Fig. 5B). When cells were treated with EM-2 for 6 h, p-AKT Ser473 and p-AKT Thr308 levels decreased and reached their lowest levels at 24 h. Downstream proteins p-GSK3β and p-FOXO3 showed a similar decreasing trend. p21 and p27 levels increased at 3 h and peaked at 9 h.

Additionally, MDA-MB-231 cells were cultured with increasing concentrations of EM-2 (0, 2, 4, 8 μM) for 24 h, and Western blotting was performed to assess expression of autophagy-related proteins (Fig. 5C). Expression levels of p62 increased with higher EM-2 concentrations, while the LC3 II/LC3 I ratio remained largely unchanged, indicating that EM-2 blocked the autophagic flux without affecting the initiation phase of autophagy. In the subsequent time-gradient experiment, when EM-2 (5 μM) was applied to MDA-MB-231 cells, p62 expression exhibited a decreasing trend before 9 h, but gradually increased after 12 h. This may be attributed to cells initiating autophagy to survive when exposed to external stimuli, however, the autophagy-blocking effect of EM-2 was enhanced after 9 h, whereas the expression of LC3 I and LC3 II did not change significantly (Fig. 5D). These results indicate that EM-2 is a dual inhibitor of the AKT pathway and autophagy.

EM-2 combined with CBP inhibits the AKT pathway and autophagy while induced apoptosis

Analysis of these findings suggests that EM-2 inhibits the AKT pathway and blocks autophagic flux, thereby enhancing the inhibitory

effect of CBP on breast cancer proliferation. As shown in Fig. 6A, expression levels of p-AKT Ser473 and p-AKT Thr308 in the EM-2+CBP group were significantly lower than that those in the CBP group, and the expression levels of downstream AKT pathway proteins p-GSK3β, p-FOXO3, and p-MDM2 were also significantly reduced. In contrast, the expression levels of p21 and p27 were significantly higher in the EM2 + CBP group compared to the CBP group. As shown in Fig. 6B, p62 expression in the EM-2 + CBP group was significantly higher than in the CBP group, indicating that EM-2 combined with CBP inhibits the AKT pathway and blocks autophagic flux.

A colony formation assay was performed to evaluate the anti-tumor effects of EM-2, CBP, and EM-2 + CBP. The inhibitory effect on cell proliferation was more pronounced in the EM-2 + CBP group compared to EM-2 or CBP alone (Fig. 6C). Furthermore, Western blot analysis revealed increased expression levels of apoptosis-related proteins CL-caspase 9 and CL-PARP in the EM-2 + CBP group (Fig. 6F). MDA-MB-231 cells were treated with EM-2, CBP, or EM-2 + CBP for 24 and 48 h, and apoptosis rates were assessed using Annexin V-FITC /PI double staining (Fig. 6D, E). After 24 h, the apoptosis rate in the EM-2 + CBP group increased by 16.14 % (25.38 % vs. 9.24 %) compared to the CBP group, and after 48 h, the increase was 22.8 % (52.6 % vs. 29.8 %). Similar results were observed in the EdU assay, with the EM-2 + CBP group showing significantly stronger inhibition of cell proliferation compared to the CBP or EM-2 groups (Fig. 6G). In addition, EM-2 sensitization to CBP was more effective than AKT or autophagy inhibitors alone and even more effective than combined inhibition of both AKT and autophagy (Fig. 6H).

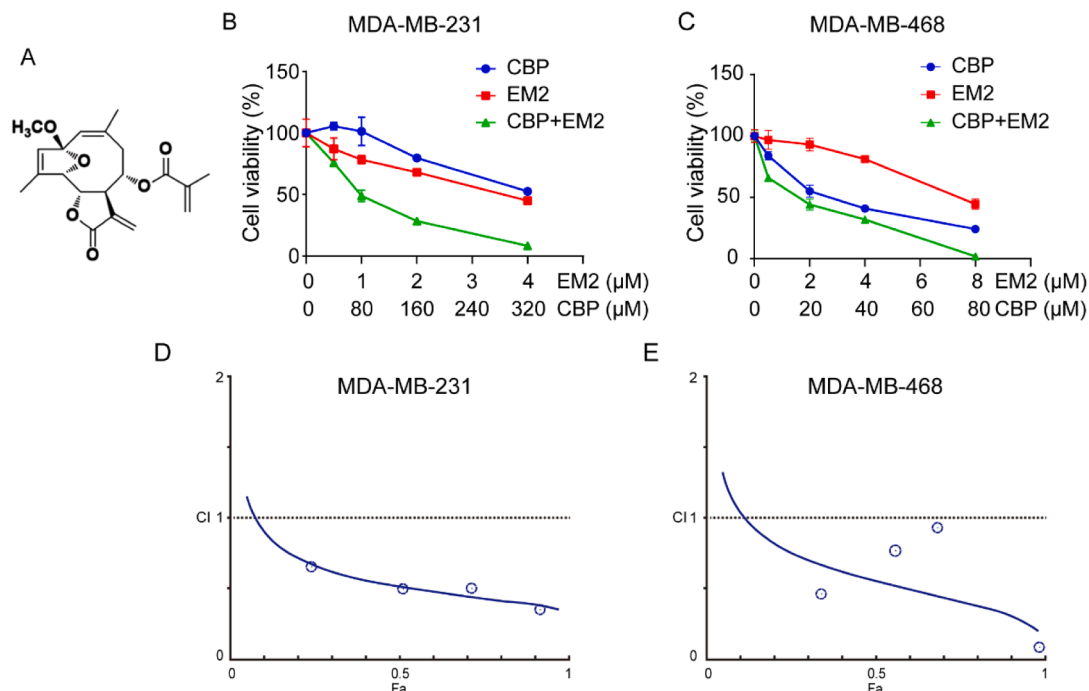


Fig. 4. Proliferation inhibition of EM-2 / CBP / EM-2 + CBP on TNBC cells. **(A)** Molecular structure of EM-2. **(B)** MDA-MB-231 and **(C)** MDA-MB-468 cells were treated with increasing concentrations of EM-2, CBP or EM-2 + CBP for 48 h, and cell viability was detected using a MTT assay. **(D)** and **(E)** Combination index (CI) was calculated using CompuSyn software.

EM-2 enhances the anti-breast cancer effect of CBP *in vivo*

MDA-MB-231 cells were used to establish a breast tumor xenograft model. When tumor volumes reached approximately 100 mm³, mice were randomly assigned to five groups: normal saline, EM-2 (6 mg/kg), CBP (16 mg/kg), EM-2 (6 mg/kg) + CBP (16 mg/kg), and EM-2 (6 mg/kg) + CBP (3 mg/kg). Treatments were administered for 21 days. Tumor volume was inhibited in the EM-2 (6 mg/kg) and CBP (16 mg/kg) groups, though the effect was modest (Fig. 7A, B, and D). A more pronounced inhibitory effect was observed in the EM-2 (6 mg/kg) + CBP (16 mg/kg) group compared to the control group. Notably, the EM-2 (6 mg/kg) + CBP (3 mg/kg) and CBP (16 mg/kg) groups had nearly the same inhibitory effect on tumor volume, indicating that the use of EM-2 combined with CBP could reduce CBP dosage. Mean tumor weight corroborated the tumor volume findings (Fig. 7C). Toxicity of EM-2, CBP, and their combination was assessed in nude mouse xenograft models. The weight change trends of mice in the five treatment groups were similar, and the toxicity of each treatment was negligible (Fig. 7E). Subsequently, immunohistochemical hematoxylin and eosin (H&E) staining was used to analyze tissue damage in the major organs of each treatment group, and the results showed no significant damage to the heart, lung, liver, spleen, and kidney in any treatment group (Fig. 7G).

The staining of Ki67 was decreased in all treatment groups compared with the control group, and was most evident in the EM-2 (6 mg/kg) + CBP (16 mg/kg) group, as shown in Fig. 7F. p62 expression serves as an indicator of autophagy. Autophagy was activated in the CBP group compared to the control group, as evidenced by a slight reduction in p62 expression in tissue sections. Conversely, p62 expression was higher in the combined treatment group than in the control group, suggesting that EM-2 inhibited CBP-induced autophagy *in vivo*. In addition, immunohistochemical analysis revealed significantly increased expression levels of p-AKT Thr308 and p-AKT Ser473 in tumors treated with CBP alone compared with control tumors; however, these expression levels decreased following the combination of CBP with EM-2 (Fig. 7F), indicating that EM-2 inhibited CBP-induced activity of the AKT pathway *in vivo*. Therefore, these findings demonstrate the synergistic anti-tumor

effect and underlying mechanism of EM-2 combined with CBP in TNBC *in vivo*.

Discussion

TNBC exhibits the highest recurrence and mortality rates among breast cancer subtypes. The standard systemic treatment for operable TNBC has relied on anthracyclines plus cyclophosphamide, followed or preceded by taxane (AC-T), due to the absence of conventional targeted therapies. Consequently, non-selective chemotherapy remains the primary approach [1]. Platinum drugs are cytotoxic DNA damage compounds that can cause DNA strand breakage and apoptosis. This mechanism of action renders them particularly effective against cancer cells with defective DNA repair, such as those with deleterious BRCA mutations. The combination of CBP with AKT inhibitors has demonstrated robust antitumor effects across various solid tumors [17–21, 47]; however, AKT inhibitors have disadvantages, such as active protective autophagy.

Transcriptome sequencing data from TCGA database revealed significantly elevated AKT1 mRNA levels in breast cancer tissues compared to normal tissues (Fig. 1A). Matching analyses further indicated overexpression of AKT1 in cancer tissues relative to paired adjacent breast tissues (Fig. 1B). Moreover, survival analysis showed that high AKT1 expression was associated with shorter overall survival (Fig. 1C). The PI3K/AKT/mTOR signaling pathway, one of the most frequently activated pathways in cancer, drives tumor cell proliferation and many other malignant behaviors [26, 48]. AKT, a key molecule in this pathway, regulates cell survival, cell growth, cell cycle regulation, and metabolism. Its anti-apoptotic function is activated when stress induces cell death [26]. The combination of AKT inhibition and chemotherapy (acting as a stress inducer) has been studied and proven to be synergistic in preclinical studies [17, 18, 47, 49]. In this study, activation of the AKT signaling pathway was observed in MDA-MB-231 cells following CBP treatment (Fig. 2A). Inhibition of the AKT pathway was found to enhance the cytotoxic effect of CBP (Fig. 2B, C, D). Furthermore, p62 levels in the CBP + LY49002 group were lower than those in

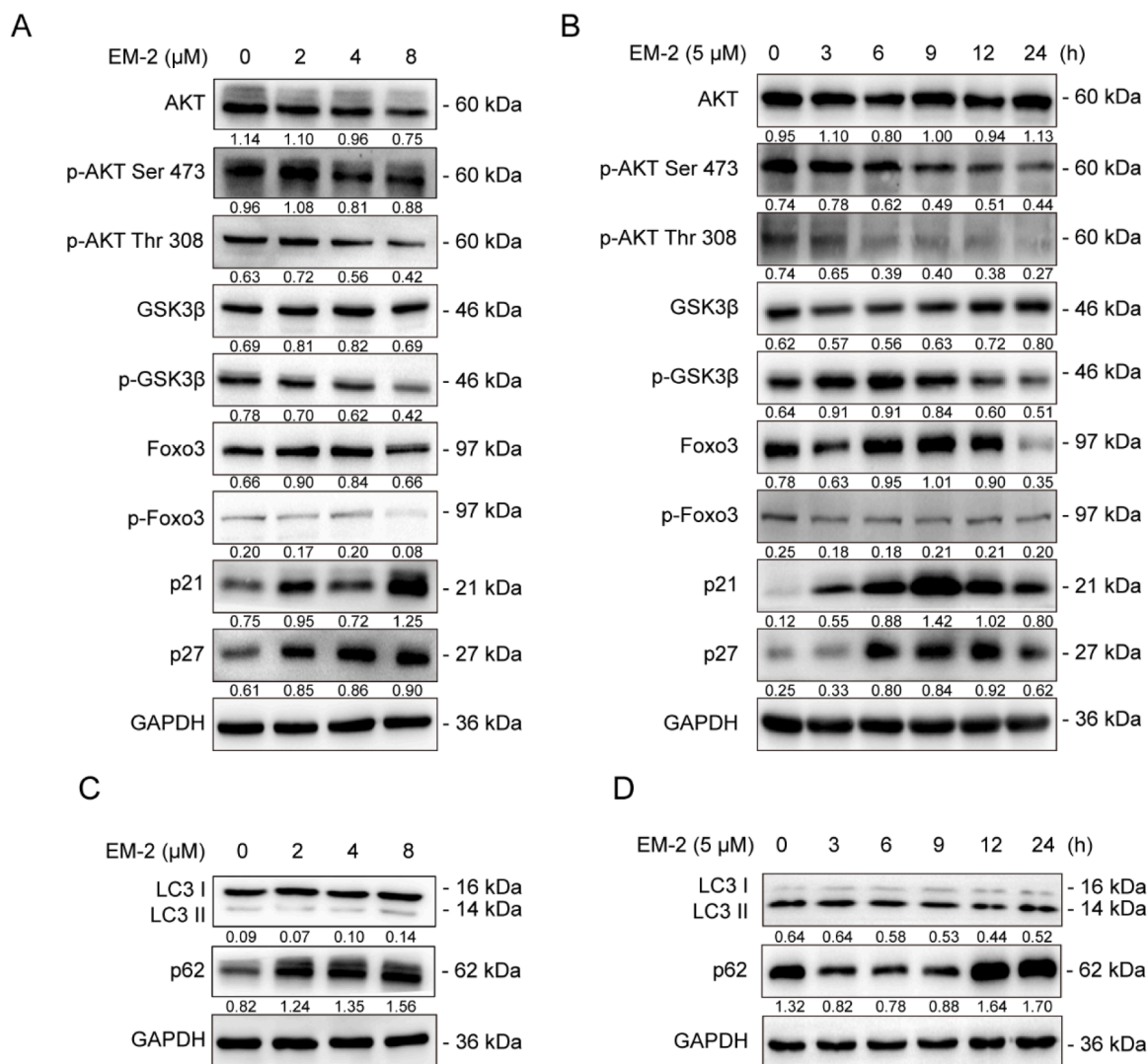
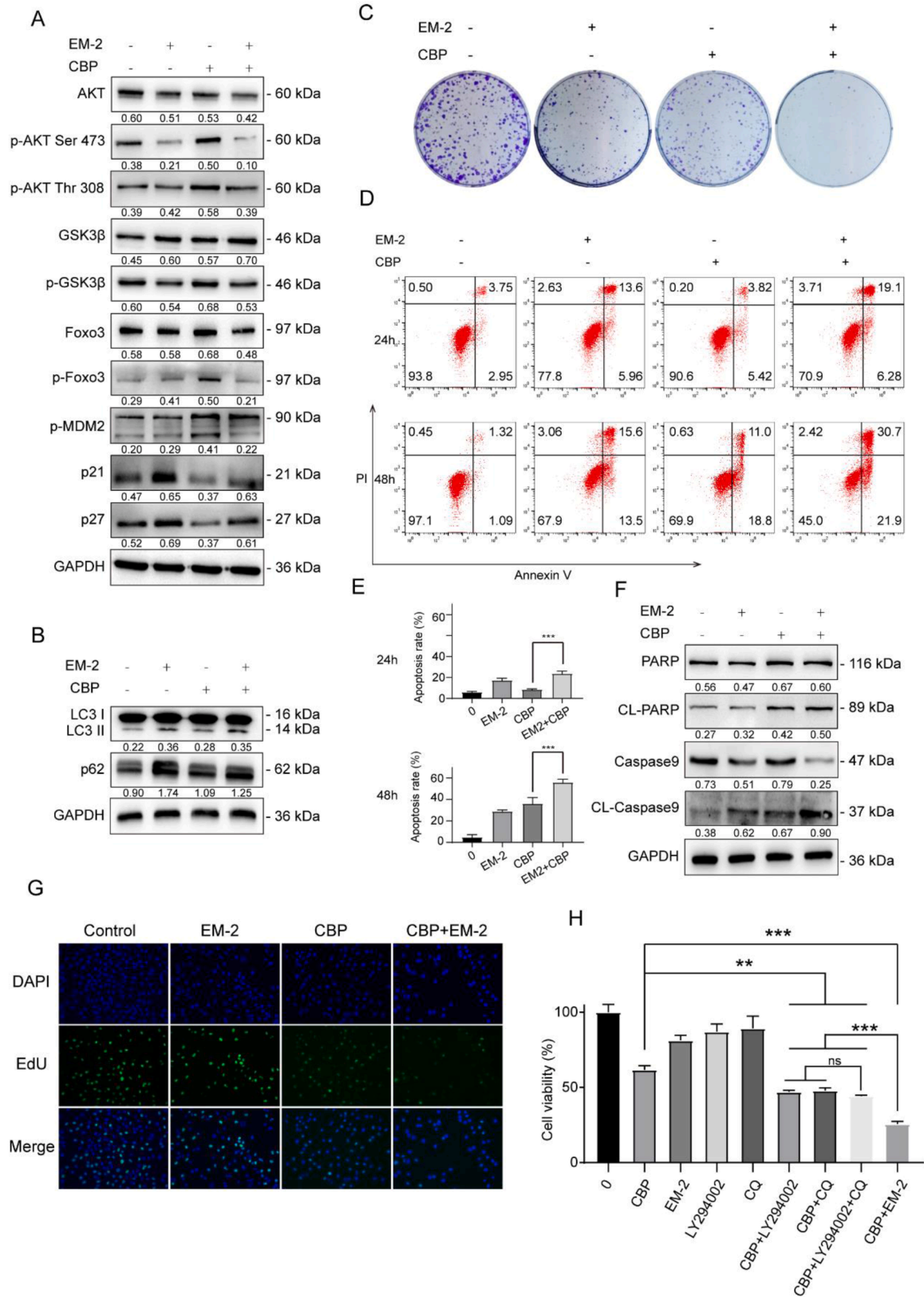


Fig. 5. EM-2 inhibits the AKT pathway and autophagic flux in a time- and dose-dependent manner. **(A)** MDA-MB-231 cells were treated with EM-2 (0, 2, 4, 8 μM, 24 h), and Western blot analysis was performed to assess expression levels of AKT pathway-associated proteins. **(B)** MDA-MB-231 cells were treated with 5 μM EM-2 for 0, 3, 6, 9, 12, and 24 h, and Western blot analysis was performed to evaluate expression levels of AKT pathway-associated proteins. **(C)** MDA-MB-231 cells were treated with EM-2 at concentrations of 0, 2, 4, or 8 μM for 24 h, and expression levels of autophagy-related proteins were assessed using Western blot analysis. **(D)** MDA-MB-231 cells were treated with 5 μM EM-2 for 0, 3, 6, 9, 12, and 24 h, and Western blot analysis was performed to determine expression levels of autophagy-associated proteins.

the CBP alone group, indicating that autophagy was activated when the AKT pathway was inhibited (Fig. 2B). However, multiple studies have shown that common PI3K-AKT/mTOR inhibitors can induce autophagy in various preclinical models, facilitating an escape from their antitumor effect [50–53]. To further investigate the effect of CBP on the autophagy pathway, cells were treated with varying concentrations of CBP. The results showed that p62 expression decreased with increasing CBP concentration, indicating autophagy activation. When the autophagy-blocking agents CQ or Baf A1 were added, the killing effect of CBP on MDA-MB-231 cells was enhanced (Fig. 3). Thus, CBP can induce protective autophagy, and inhibition of autophagy can increase its anti-tumor effect.

Given these observations, the potential dual inhibition of AKT and autophagy in combination with CBP was considered to enhance anti-tumor efficacy while reducing CBP dosage and associated toxic side effects. Natural products have been widely utilized in tumor treatment due to their advantages, including low cytotoxicity, high efficiency, and low cost. In this study, sesquiterpene lactone monomer EM-2 extracted from *Elephantopus mollis* H.B.K., was identified (Fig. 5). Following EM-2

treatment, the expression levels of p-AKT Ser473 and p-AKT Thr308 proteins decreased, and the phosphorylation levels of the downstream proteins GSK3β and FOXO3 also decreased, indicating that EM-2 inhibited the AKT pathway. The protein expression of p62 increased with increasing EM-2 concentration, indicating that EM-2 inhibited autophagy (Fig. 5C, D). CBP combined with EM-2 exhibited a synergistic anti-TNBC effect ($CI < 1$) (Fig. 4D, E). Further investigation revealed that the apoptosis rates in the EM-2 + CBP group increased by 16.14% (25.38% vs. 9.24%) after 24 h and by 22.8% (52.6% vs. 29.8%) after 48 hours compared to the CBP-alone group (Fig. 6D, E). In addition, colony formation and EdU assays demonstrated that CBP combined with EM-2 inhibited cell proliferation (Fig. 6C, G). Notably, the synergistic antitumor effects of CBP and EM-2 could not be replicated by simply adding AKT and autophagy inhibitors (Fig. 6H). In further study, we constructed MDA-MB-231 breast tumor xenograft models to explore the synergistic anti-tumor effects of CBP combined with EM-2 *in vivo*. Consistent with the *in vitro* experiments, the combination of EM-2 (6 mg/kg) with approximately one-fifth the concentration (3 mg/kg) of CBP exhibited similar antitumor effects as the CBP (16 mg/kg) alone



(caption on next page)

Fig. 6. EM-2 combined with CBP inhibits the AKT pathway and autophagic flux while inducing apoptosis. **(A)** MDA-MB-231 cells were treated with CBP (400 μ M, 24 h) with or without EM-2 (5 μ M, 24 h), and Western blot analysis was performed to assess expression levels of AKT pathway-associated proteins. **(B)** MDA-MB-231 cells were treated with CBP (400 μ M, 24 h) with or without EM-2 (5 μ M, 24 h), and the proteins related to autophagy were detected using Western blot analysis. **(C)** MDA-MB-231 cells were treated with EM-2 (0.25 μ M), CBP (2.5 μ M), or EM-2 (0.25 μ M) + CBP (2.5 μ M) for 7 days, followed by a colony formation assay. **(D)** MDA-MB-231 cells were treated with EM-2 (5 μ M), CBP (400 μ M), or EM-2 (5 μ M) + CBP (400 μ M) for 24 h or 48 h, and apoptosis rates were measured using flow cytometry, with DMSO (0.02 % maximum volume ratio) as the control. **(E)** Percentage of apoptotic cells (mean \pm SD for three trials) (** P < 0.01, *** P < 0.001). **(F)** MDA-MB-231 cells were treated with EM-2 (5 μ M), CBP (400 μ M) or EM-2 (5 μ M) + CBP (400 μ M) for 24 h, and the apoptosis-related proteins were detected using Western blot analysis. **(G)** The inhibitory effect of CBP (200 μ M, 24 h), with or without EM-2 (2 μ M, 24 h), on MDA-MB-231 cells was evaluated using an EdU assay and DMSO (0.02 % maximum volume ratio) as the control. **(H)** MDA-MB-231 cells were treated with CBP (400 μ M), EM-2 (2 μ M), LY294002(10 μ M), CQ (10 μ M), CBP (400 μ M) + LY294002(10 μ M), CBP (400 μ M) + CQ (10 μ M), CBP (400 μ M) + LY294002(10 μ M) + CQ (10 μ M) or CBP (400 μ M) + EM-2 (2 μ M) for 24 h, and MTT analysis was used to detect the cell viability (** P < 0.01, *** P < 0.001).

group (Fig. 7A, B, C), indicating that EM-2 combined with CBP can reduce the required CBP dosage. Moreover, immunohistochemical analysis revealed that EM-2 inhibits the AKT pathway and autophagy *in vivo* (Fig. 7F).

These findings demonstrated that EM-2 combined with CBP exhibits synergistic anti-TNBC activity *in vivo* and *in vitro* (Fig. 8).

Conclusion

This study revealed that the AKT pathway is activated following CBP treatment of TNBC cells and that inhibition of this pathway enhances the anti-tumor effect of CBP. Autophagy was found to be induced by CBP, either alone or in combination with AKT inhibitors, and blocking autophagy amplified the anti-tumor efficacy of CBP. EM-2 is a natural small-molecule compound that inhibits both the AKT pathway and autophagy. The combination of EM-2 with CBP exhibited a synergistic anti-tumor effect and promoted apoptosis, a finding further validated *in vivo*.

Materials and methods

Chemicals and reagents

EM-2 was identified by Professor Wang Guocai at the College of Pharmacy, Jinan University (Guangzhou, China)[54]. Its purity was determined to be \geq 95 % by high-performance liquid chromatography. EM-2 was dissolved in dimethyl sulfoxide (DMSO), aliquoted, and stored at -80 °C.

The Annexin V-FITC apoptosis detection kit, MTT cell proliferation assay kit, and kFluor488-EdU detection kit were obtained from KeyGEN Biotech (Jiangsu, China). Bafilomycin A1 (Baf-A1), chloroquine (CQ), LY294002, and Triciribine were sourced from Selleck (Houston, TX, USA). The Immobilion electrochemiluminescence (ECL) kit and polyvinylidene fluoride (PVDF) were acquired from Millipore (MA, USA). Antibodies against Caspase-9, CL-Caspase-9, poly ADP-ribose polymerase (PARP), CL-PARP, AKT, p-AKT Thr308, p-AKT Ser473, GSK3 β , p-GSK3 β , FOXO3, p-FOXO3, MDM2, p-MDM2, p21, p27, p62, LC3 I/II, and GAPDH were purchased from Cell Signaling Technology (Boston, MA). Goat anti-mouse IgG(H + L) and goat anti-rabbit IgG(H + L) antibodies were obtained from Proteintech.

Cell culture

MDA-MB-231, and MDA-MB-468 cells, acquired from the American Type Culture Collection, were cultured in DMEM high-glucose medium supplemented with 10 % fetal bovine serum (FBS). Cells were cultured at 37 °C in an atmosphere containing 5 % CO₂.

Cell viability assay

Cells were seeded into 96-well plates at a density of 5000 cells per well and incubated overnight at 37 °C in a 5 % CO₂ atmosphere. Subsequently, cells were treated with various agents for 24 or 48 h. MTT solution (20 μ L per well) was introduced into the culture plates followed

by a 4-h incubation at 37 °C. Following supernatant removal, DMSO (150 μ L per well) was added, and absorbance was measured at 570 nm using a microplate spectrophotometer (Bio-Rad Laboratories, Hercules, CA, USA). The experiments were conducted in triplicate.

EdU staining assay

Cells were seeded into 96-well plates at a density of 6000 cells per well and treated with 0.02 % DMSO (control group) or corresponding drugs. EdU staining assays were performed to detect cell proliferation using the kFluor488-EdU detection kit (KeyGEN, Jiangsu, China), according to the manufacturer's instructions.

Colony formation assay

MDA-MB-231 cells in logarithmic growth phase were seeded into six-well plates (1000 cells/well) and incubated overnight at 37 °C in a 5 % CO₂ atmosphere. Cells were then treated with varying concentrations of EM-2, CBP, or their combination for 7 days. After fixation with 4 % paraformaldehyde for 20 min, colonies were stained with 0.5 % crystal violet solution (Sigma, USA) for 30 min. Following gentle rinsing and drying, colonies were counted and imaged.

Apoptosis analysis

Apoptosis was evaluated using an Annexin V-FITC detection system (KeyGEN Biotech) according to the manufacturer's specifications. Cells were seeded in six-well plates at 2.0×10^5 cells/well and treated with drugs for 24 or 48 h. Cells were harvested, washed with PBS, and resuspended in binding buffer. Annexin V-FITC (5 μ L) and propidium iodide (5 μ L) were added, followed by 30-min dark incubation at 25 °C. Flow cytometric analysis was performed (Becton, Dickinson and Company, VT).

Western blot

Cells were seeded in six-well plates (2.0×10^5 cells/well) and treated with drugs for 24 h. Proteins were extracted using RIPA buffer (Cell Signaling Technology, MA, USA). The lysate underwent centrifugation ($12,000 \times g$, 15 min, 4 °C) to isolate protein supernatants. Protein concentration was quantified using a BCA assay (Sangon Biotech, China). Following SDS-PAGE separation and PVDF membrane (Millipore, Billerica, MA, USA) transfer, membranes underwent blocking with 5 % non-fat milk (1 h, room temperature), primary antibody incubation (overnight, 4 °C), and secondary antibody treatment (1.5 h, room temperature). After washing with TBST, proteins were visualized using ECL substrate and a gel documentation system (UVItec Ltd., Cambridge, UK).

Xenograft experiments

Animal protocols were approved by the IACUC of Jinan University (IACUC-20,220,425-03). Female BALB/c nude mice (5-6 weeks, Guangdong Yaokang) were subcutaneously injected with MDA-MB-231 cells (5×10^6 cells/mouse). When tumors reached approximately 100

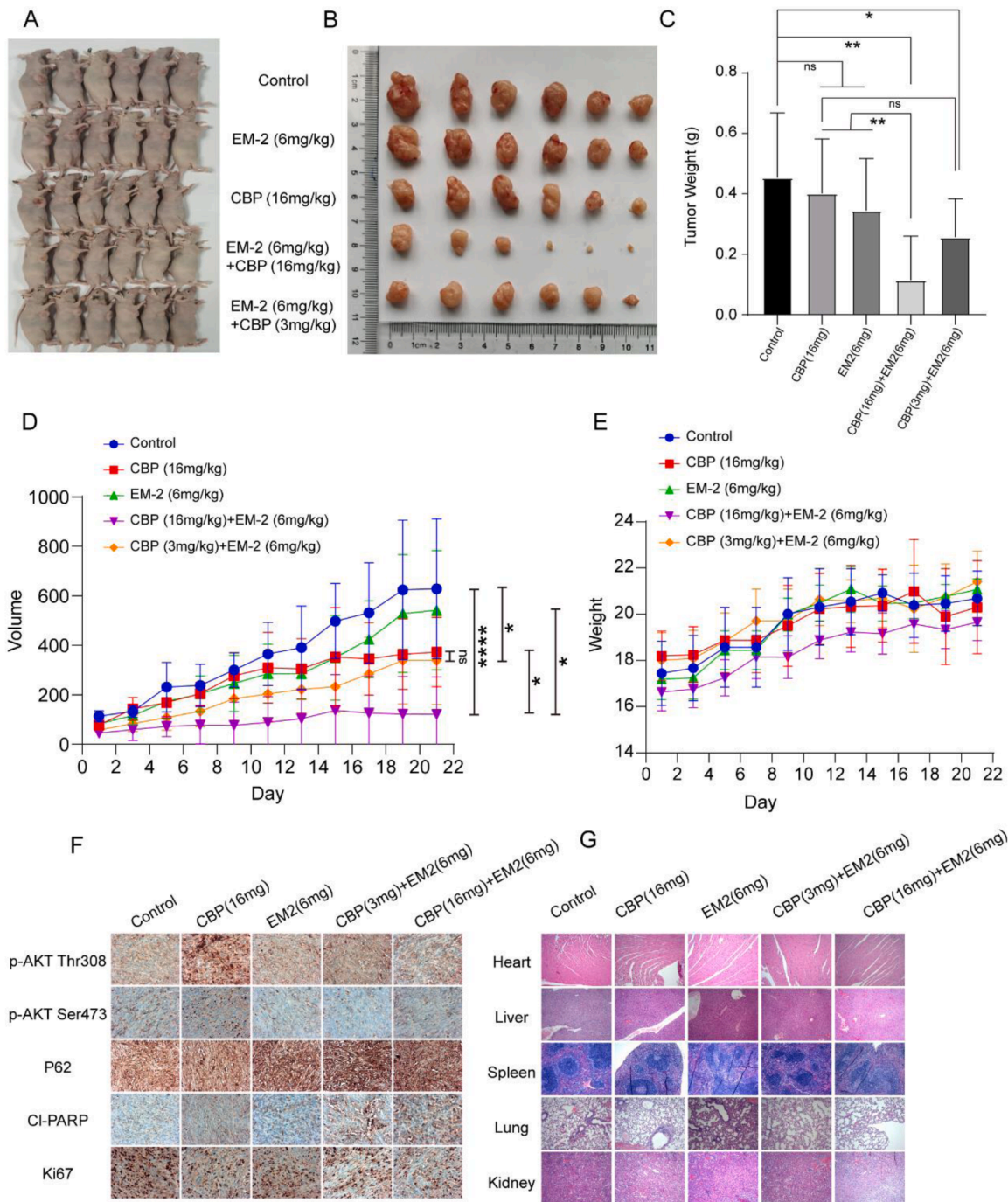


Fig. 7. EM-2 combined with CBP significantly inhibits tumor growth in a xenograft tumor model. (A) Animals were euthanized after 21 days of administration. (B) Tumors were excised and photographed following euthanasia. (C) Tumor weights in all groups were recorded after 21 days of administration (the mean \pm SD of each group, * $P < 0.05$). (D) Tumor volumes and (E) body weights of mice in all treatment groups were measured every 2 days over 21 days. (* $P < 0.05$, ** $P < 0.01$). (F) Immunohistochemical analysis of Ki67, p62, p-AKT Thr308, p-AKT Ser473, and CL-PARP in tumor specimens harvested from mice (original magnification, $\times 200$). (G) Immunohistochemical hematoxylin and eosin (H&E) staining of heart, lung, liver, spleen, and kidney in each treatment group.

mm³, mice were randomized into five cohorts ($n = 6$): (i) saline control (i.p.); (ii) EM-2 treatment (6 mg/kg, i.p.); (iii) CBP administration (16 mg/kg, i.p.); (iv) combination therapy; and (v) reduced-dose combination (EM-2 6 mg/kg + CBP 3 mg/kg, approximately one-fifth of group iv concentration). Treatments were administered daily, and tumor dimensions [(length \times width²)/2] and body weight were monitored every two days. Terminal procedures were performed on day 21, followed by the collection of tumor and organ specimens (liver, heart, lung, spleen, and kidney) for histological and immunohistochemical analyses.

Bioinformatics analysis

Gene expression data and clinical features of patients with breast cancer were retrospectively retrieved from publicly available datasets, such as the TCGA database (portal.gdc.cancer.gov). The mRNA expression of AKT1 and autophagy-related genes in breast cancer was transformed into transcripts per kilobase million, and differential expression analyses were conducted using the Limma package (version 3.54.2)[55]. Survival analysis was performed using the survival package [56,57] and SurvMiner [58]. Optimal cutoff values were determined using the

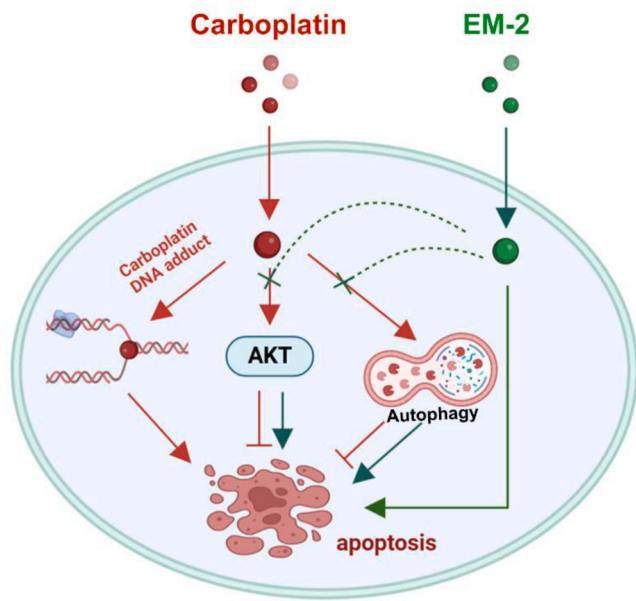


Fig. 8. Abstract graph: EM-2 sensitizes CBP by inhibiting the AKT and autophagy pathways.

surv_cutpoint function.

Statistical analysis

IBM SPSS Statistics 20, GraphPad Prism 7.0, and R 4.2.3. were used for statistical analysis. Significant differences were assessed using Student's *t*-test and one-way ANOVA. Survival analysis was assessed using the Kaplan–Meier method and log-rank test. A *P*-value < 0.05 was considered statistically significant.

CRediT authorship contribution statement

Jun-zhen Zhou: Writing – original draft, Investigation, Data curation. **Jing-ya Wen:** Writing – review & editing, Data curation. **Xin-wen Xu:** Writing – review & editing, Investigation. **Na Zhao:** Investigation, Data curation. **Jing-jing Tang:** Validation, Investigation. **Ye-rui Xiao:** Validation, Investigation. **Le-yang Xiang:** Validation, Investigation. **Yue Jiang:** Funding acquisition. **Jian-wei jiang:** Writing – review & editing, Project administration, Investigation. **Hong Hong:** Supervision, Funding acquisition. **Qing Zhang:** Investigation, Funding acquisition.

Declaration of competing interest

The authors declare that they have no competing interests.

Acknowledgements

This research was supported by Medical Joint Fund Free Application Program in Jinan University (MF220205); Medical Joint Fund Free Application Program in Jinan University (YXZY2022022); The Basic and Applied Basic Research Fund Project of Guangdong Province (2022A151540186); the Natural Science Foundation of Guangdong Province in China (2021A1515012521); the First Affiliated Hospital of Jinan University Flagship specialty construction project-General surgery (711003); Funding by Science and Technology Projects in Guangzhou (2025A03J4260).

Ethics approval and consent to participate

The animal experiment was approved by the Institutional Animal

Care and Use Committee of Jinan University.

Consent for publication

Not applicable.

Availability of data and materials

The datasets used and/or analysed during the current study are available from the corresponding author on reasonable request.

Supplementary materials

Supplementary material associated with this article can be found, in the online version, at [doi:10.1016/j.tranon.2025.102434](https://doi.org/10.1016/j.tranon.2025.102434).

References

- [1] R.A. Leon-Ferre, M.P. Goetz, Advances in systemic therapies for triple negative breast cancer, *BMJ* 381 (2023) e071674.
- [2] S. Zhu, Y. Wu, B. Song, et al., Recent advances in targeted strategies for triple-negative breast cancer, *J. Hematol. Oncol.* 16 (2023) 100.
- [3] V.B. Varzaru, T. Vlad, R. Popescu, C.S. Vlad, A.E. Moatar, I.M. Cobec, Triple-negative breast cancer: molecular particularities still a challenge, *Diagnostics* 14 (2024).
- [4] J.D. Benitez Fuentes, E. Morgan, A. de Luna Aguilar, et al., Global stage distribution of breast cancer at diagnosis: a systematic review and meta-analysis, *JAMA Oncol.* 10 (2024) 71–78.
- [5] H. Mallipeddi, A. Thyagarajan, R.P. Sahu, Implications of Withaferin-A for triple-negative breast cancer chemoprevention, *Biomed. Pharmacother.* 134 (2021) 111124.
- [6] G.K. Gupta, A.L. Collier, D. Lee, et al., Perspectives on triple-negative breast cancer: current treatment strategies, unmet needs, and potential targets for future therapies, *Cancers* 12 (2020) 2392.
- [7] I. Meattini, C. Becherini, S. Caini, et al., International multidisciplinary consensus on the integration of radiotherapy with new systemic treatments for breast cancer: european society for radiotherapy and oncology (ESTRO)-endorsed recommendations, *Lancet Oncol.* 25 (2024) e73–e83.
- [8] M.A. Harris, P. Savas, B. Virassamy, et al., Towards targeting the breast cancer immune microenvironment, *Nat. Rev. Cancer* 24 (2024) 554–577.
- [9] J.S. Lee, S.E. Yost, Y. Yuan, Neoadjuvant treatment for triple negative breast cancer: recent progresses and challenges, *Cancers* 12 (2020) 1404.
- [10] P. Chowdhury, U. Ghosh, K. Samanta, M. Jaggi, S.C. Chauhan, M.M. Yallapu, Bioactive nanotherapeutic trends to combat triple negative breast cancer, *Bioactive Mater.* 6 (2021) 3269–3287.
- [11] E.A. O'Reilly, L. Gubbins, S. Sharma, et al., The fate of chemoresistance in triple negative breast cancer (TNBC), *BBA Clin.* 3 (2015) 257–275.
- [12] Y. Zhu, Y. Hu, C. Tang, X. Guan, W. Zhang, Platinum-based systematic therapy in triple-negative breast cancer, *Biochim. Biophys. Acta. (BBA)* 1877 (2022) 188678.
- [13] K.D. Yu, F.G. Ye, M. He, et al., Effect of adjuvant paclitaxel and carboplatin on survival in women with triple-negative breast cancer: a phase 3 randomized clinical trial, *JAMA Oncol.* 6 (2020) 1390–1396.
- [14] X. Dong, X. Bai, J. Ni, et al., Exosomes and breast cancer drug resistance, *Cell Death. Dis.* 11 (2020) 987.
- [15] K. Gohr, A. Hamacher, L.H. Engelke, M.U. Kassack, Inhibition of PI3K/akt/mTOR overcomes cisplatin resistance in the triple negative breast cancer cell line HCC38, *BMC Cancer* 17 (2017) 1–13.
- [16] M. Hagiwara, E. Kikuchi, N. Tanaka, et al., Variant isoforms of CD44 involves acquisition of chemoresistance to cisplatin and has potential as a novel indicator for identifying a cisplatin-resistant population in urothelial cancer, *BMC Cancer* 18 (2018) 1–11.
- [17] W.C. Burkett, Z. Zhao, M.A. Newton, et al., Ipatasertib, an oral akt inhibitor, in combination with carboplatin exhibits anti-proliferative effects in uterine serous carcinoma, *Ann. Med.* 55 (2023) 603–614.
- [18] C.S. Lee, Y.J. Kim, E.R. Jang, S.C. Myung, W. Kim, Akt inhibitor enhances apoptotic effect of carboplatin on human epithelial ovarian carcinoma cell lines, *Eur. J. Pharmacol.* 632 (2010).
- [19] J. Chen, T. Lan, J. Hou, et al., Atorvastatin sensitizes human non-small cell lung carcinomas to carboplatin via suppression of akt activation and upregulation of TIMP-1, *Int. J. Biochem. Cell Biol.* 44 (2012) 759–769.
- [20] A. Leary, P. Estévez-García, R. Sabatier, et al., ENDOLUNG trial. a phase 1/2 study of the akt/mTOR inhibitor and autophagy inducer Ibrilatazar (ABTL0812) in combination with paclitaxel/carboplatin in patients with advanced/recurrent endometrial cancer, *BMC Cancer* 24 (2024) 876.
- [21] Y. Dong, T. Xu, D. Li, et al., NLR family card domain containing 5 promotes hypoxia-induced cancer progress and carboplatin resistance by activating PI3K/AKT via carcinoembryonic antigen related cell adhesion molecule 1 in non-small cell lung cancer, *Bioengineered* 13 (2022) 14413–14425.
- [22] L. Rong, Z. Li, X. Leng, et al., Salidroside induces apoptosis and protective autophagy in human gastric cancer AGS cells through the PI3K/akt/mTOR pathway, *Biomed. Pharmacother.* 122 (2020) 109726.

- [23] A. Glaviano, A.S.C. Foo, H.Y. Lam, et al., PI3K/AKT/mTOR signaling transduction pathway and targeted therapies in cancer, *Mol. Cancer* 22 (2023) 138.
- [24] G. Hoxhaj, B.D. Manning, The PI3K–AKT network at the interface of oncogenic signalling and cancer metabolism, *Nat. Rev. Cancer* 20 (2020) 74–88.
- [25] S. Capici, L.C. Ammoni, N. Meli, et al., Personalised therapies for metastatic triple-negative breast cancer: when target is not everything, *Cancers* 14 (2022).
- [26] J. Pascual, N.C. Turner, Targeting the PI3-kinase pathway in triple-negative breast cancer, *Ann. Oncol.* 30 (2019) 1051–1060.
- [27] Comprehensive molecular portraits of human breast tumours, *Nature* 490 (2012) 61–70.
- [28] M. Falasca, PI3K/Akt signalling pathway specific inhibitors: a novel strategy to sensitize cancer cells to anti-cancer drugs, *Curr. Pharm. Des.* 16 (2010) 1410–1416.
- [29] F. Rascio, F. Spadaccino, M.T. Rocchetti, et al., The pathogenic role of PI3K/AKT pathway in cancer onset and drug resistance: an updated review, *Cancers* 13 (2021) 3949.
- [30] I.M. Browne, F. André, S. Chandralapaty, L.A. Carey, N.C. Turner, Optimal targeting of PI3K-AKT and mTOR in advanced oestrogen receptor-positive breast cancer, *Lancet Oncol.* 25 (2024) e139–e151.
- [31] H.T. Wu, J. Lin, Y.E. Liu, et al., Luteolin suppresses androgen receptor-positive triple-negative breast cancer cell proliferation and metastasis by epigenetic regulation of MMP9 expression via the AKT/MTOR signaling pathway, *Phytomedicine* 81 (2021) 153437.
- [32] Y. Li, S. Hu, Y. Chen, et al., Calycosin inhibits triple-negative breast cancer progression through down-regulation of the novel estrogen receptor- α splice variant ER- α 30-mediated PI3K/AKT signaling pathway, *Phytomedicine* 118 (2023) 154924.
- [33] B. Markman, R. Dienstmann, J. Tabernero, Targeting the PI3K/Akt/mTOR pathway—beyond rapalogs, *Oncotarget* 1 (2010) 530.
- [34] C.K. Cheng, Q.W. Fan, W.A. Weiss, PI3K signaling in glioma—Animal models and therapeutic challenges, *Brain Pathol.* 19 (2009) 112–120.
- [35] C.W. Yun, S.H. Lee, The roles of autophagy in cancer, *Int. J. Mol. Sci.* 19 (2018) 3466.
- [36] I. Daskalaki, I. Gkikas, N. Tavernarakis, Hypoxia and selective autophagy in cancer development and therapy, *Front. Cell Dev. Biol.* 6 (2018) 104.
- [37] R. Chavez-Dominguez, M. Perez-Medina, J.S. Lopez-Gonzalez, M. Galicia-Velasco, D. Aguilar-Cazares, The double-edge sword of autophagy in cancer: from tumor suppression to pro-tumor activity, *Front. Oncol.* 10 (2020) 578418.
- [38] T.Y. Chen, B.M. Huang, T.K. Tang, et al., Genotoxic stress-activated DNA-PK-p53 cascade and autophagy cooperatively induce ciliogenesis to maintain the DNA damage response, *Cell Death Differ.* 28 (2021) 1865–1879.
- [39] D. Zhang, J. Pan, X. Xiang, et al., Protein kinase c δ suppresses autophagy to induce kidney cell apoptosis in cisplatin nephrotoxicity, *J. Am. Soc. Nephrol.* 28 (2017) 1131–1144.
- [40] Y. Jiang, F. Ji, Y. Liu, et al., Cisplatin-induced autophagy protects breast cancer cells from apoptosis by regulating yes-associated protein, *Oncol. Rep.* 38 (2017) 3668–3676.
- [41] S. Cocco, M. Piezzo, A. Calabrese, et al., Biomarkers in triple-negative breast cancer: state-of-the-art and future perspectives, *Int. J. Mol. Sci.* 21 (2020).
- [42] S.Y. Park, J.H. Choi, J.S. Nam, Targeting cancer stem cells in triple-negative breast cancer, *Cancers* 11 (2019).
- [43] T. Jiang, J. Zhu, S. Jiang, et al., Targeting lncRNA DDIT4-AS1 sensitizes triple negative breast cancer to chemotherapy via suppressing of autophagy, *Adv. Sci.* 10 (2023) e2207257.
- [44] S. Cocco, A. Leone, M.S. Roca, et al., Inhibition of autophagy by chloroquine prevents resistance to PI3K/AKT inhibitors and potentiates their antitumor effect in combination with paclitaxel in triple negative breast cancer models, *J. Transl. Med.* 20 (2022) 290.
- [45] Y. Ichimura, T. Kumanomidou, Y-s Sou, et al., Structural basis for sorting mechanism of p62 in selective autophagy, *J. Biol. Chem.* 283 (2008) 22847–22857.
- [46] R.K. Amaravadi, A.C. Kimmelman, J. Debnath, Targeting autophagy in cancer: recent advances and future directions, *Cancer Discov.* 9 (2019) 1167–1181.
- [47] Y.H. Lin, B.Y. Chen, W.T. Lai, et al., The AKT inhibitor MK-2206 enhances the cytotoxicity of paclitaxel (Taxol) and cisplatin in ovarian cancer cells, *Naunyn Schmiedebergs Arch. Pharmacol.* 388 (2015) 19–31.
- [48] N. Dey, P. De, B. Leyland-Jones, PI3K-AKT-mTOR inhibitors in breast cancers: from tumor cell signaling to clinical trials, *Pharmacol. Ther.* 175 (2017).
- [49] X. Song, H. Cai, Z. Shi, et al., Enzyme-responsive branched glycopolymer-based nanoassembly for co-delivery of paclitaxel and AKT inhibitor toward synergistic therapy of gastric cancer, *Adv. Sci.* 11 (2024) e2306230.
- [50] Y. Wang, J. Liu, Y. Qiu, et al., ZSTK474, a specific class I phosphatidylinositol 3-kinase inhibitor, induces G1 arrest and autophagy in human breast cancer MCF-7 cells, *Oncotarget* 7 (2016) 19897–19909.
- [51] C. Amaral, T.V. Augusto, E. Tavares-da-Silva, F.M.F. Roleira, G. Correia-da-Silva, N. Teixeira, Hormone-dependent breast cancer: targeting autophagy and PI3K overcomes exemestane-acquired resistance, *J. Steroid Biochem. Mol. Biol.* 183 (2018) 51–61.
- [52] Y. Ji, W. Di, Q. Yang, Z. Lu, W. Cai, J. Wu, Inhibition of autophagy increases proliferation inhibition and apoptosis induced by the PI3K/mTOR inhibitor NVP-BEZ235 in breast cancer cells, *Clin. Lab.* 61 (2015) 1043–1051.
- [53] Y.C. Kim, K.L. Guan, mTOR: a pharmacologic target for autophagy regulation, *J. Clin. Invest.* 125 (2015) 25–32.
- [54] Z.N. Wu, Y.B. Zhang, N.H. Chen, et al., Sesquiterpene lactones from *elephantopus mollis* and their anti-inflammatory activities, *Phytochemistry* 137 (2017) 81–86.
- [55] B. Phipson, S. Lee, L.J. Majewski, W.S. Alexander, G.K. Smyth, Robust hyperparameter estimation protects against hypervariable genes and improves power to detect differential expression, *Ann. Appl. Stat.* 10 (2016) 946–963.
- [56] Therneau T. A package for survival analysis in R. R package version 3.2-7. 2020. URL <https://CRAN.R-project.org/package=survival>.2021.
- [57] T.M. Therneau, P.M. Grambsch, T.M. Therneau, P.M. Grambsch, *The Cox Model*, Springer, 2000.
- [58] A. Kassambara, M. Kosinski, P. Hsieh, S. Fabian, survminer: Drawing Survival Curves using ggplot2, R package version 0.4. 9. 2021, 2021.